Ellipsometric characterization of Bi and Al_2O_3 coatings for plasmon excitation in an optical fiber sensor

Running title: Characterization of Bi and Al_2O_3 for plasmonic sensor

Running Authors: E. Rodríguez-Schwendtner et al.

Eva Rodríguez-Schwendtner[1], Alberto Álvarez-Herrero[2], Antonio Mariscal[3], Rosalía Serna[3], Agustín González-Cano[1,a)], María-Cruz Navarrete[4] and Natalia Díaz-Herrera[1]

[1] Applied Optics Complutense Group, Complutense University, Faculty of Optics and Optometry, Arcos de Jalón 118, 28037 Madrid (Spain)
[2] Space Optics Area, Instituto Nacional de Técnica Aerospacial (INTA), Ctra. de Ajalvir, km. 4, 28850 Torrejón de Ardoz, Madrid (Spain)
[3] Laser Processing Group, Instituto de Óptica CSIC, Serrano 121, 28006 Madrid (Spain)
[4] Applied Optics Complutense Group, Complutense University, Faculty of Physics, Plaza de Ciencias 1, Ciudad Universitaria, 28040 Madrid (Spain)

[a)] Electronic mail: agugonza@ucm.es

We present the results of the ellipsometric characterization of thin layers of Bismuth (Bi) and Aluminum Oxide (Al_2O_3) deposited over the waist of a tapered optical fiber by Pulsed Laser Deposition (PLD). The characteristics of the deposits are studied by spectroscopic ellipsometry. From the effective thicknesses determined by the ellipsometric characterization it is shown by simulations that surface plasmon resonances can occur in the fiber device, and it is demonstrated experimentally. These results show the feasibility of employing Bismuth as a plasmonic material in SPR fiber sensors based on Doubly-deposited Uniform-waist Tapered optical fibers (DLUWTs), which show excellent performance and versatility.

I. INTRODUCTION

Bismuth is a semimetal that has attracted a continuous interest in research during much of the 20th century due to its characteristic band structure that enables special properties including diamagnetism, Haas-Van de Alphen effect, low thermal conductivity, high thermoelectrical coefficient, superconductivity and strongly coupled electron-plasmon “plasmaron" features in the far infrared (IR) among others.[1,2] Optical spectroscopy studies have demonstrated to be essential to understand the electronic properties of Bi in bulk, thin films and nanostructures such as nanocrystals and nanowires. The earliest data were reported in the 60’s by Cardona and Greenaway[3] and consisted of reflectivity and absorption measurements that were analized using the Kramers-Kronig relationship. A decade later, in 1975, Hunderei reported the first ellipsometry measurements in the visible that enabled the first relevant picture of the electronic structure of bulk Bi.[4] These early works were soon followed by photoemision spectroscopy studies in the 90’s that helped to complete the information on its energy levels.[5] More recently in the 21st century the interest on the electronic properties of Bi has broadened, in relationship with spintronics with the discovery of spin dependent properties of Bi surfaces, and within the area of plasmonics. In the latter case it has been demonstrated that Bi nanostructures show surface plasmon-like resonances in the visible-UV spectra region.[6-8] Detailed spectroscopic ellipsometry investigations have suggested that in the case of Bi the plasmonic behavior is induced by different elemental mechanisms in the ultraviolet-visible and infrared range, namely by the excitation of interband transitions and the excitation of free carriers, respectively. [9-11] The use of interband transitions is very attractive because it opens the way to the achievement of visible-UV plasmonic properties without free carriers that could be tunable through the tailoring of the band structure of the materials and the occupation of electronic states.

As it is well known, plasmonics is a key technique to produce very sensitive optical sensors, mostly based in the strong dependence of the mechanism of plasmon excitation with the refractive index of the medium surrounding the sensing region in the so-called Surface Plasmon Resonance (SPR) devices.[12,13] Nowadays, plasmonic sensors have become a standard in the realm of chemical analysis and biosensors.[14] Among the many possibilities and varieties of plasmonic optical sensors, those based on optical fibers add to the good performance of SPR devices other aspects such as accessibility to remote or hazardous places for in situ measurements, small size, robustness, multiplexing, etc. Many SPR fiber sensors have been proposed.[15] For years, we have been working in the so-called DLUWTs (doubly-deposited uniform-waist optical fibers), structures in which a double deposit (metal plus dielectric) is deposited on a tapered optical fiber. The tapering makes the evanescent field accessible and the fact that there are two layers permits not only the excitation of the plasmon but also the tuning of its position in terms of resonance wavelength. We have proven that starting with the same configuration and changing only the thicknesses of the materials employed we can cover from the middle of the visible spectrum to the optical communications region.[16-18] Different materials for the dielectric layer have also been considered[19].

DLUWTs are powerful refractometers, with high values of sensitivity[20]. This fact can be employed in the usual way, in chemical and biological sensors, or, as we have recently proven, also in physical sensors to measure magnetic fields using ferrofluids as transducers.[21-22]

In this work we combine the above depicted properties of Bi with the versatility and proved good performance of DLUWTs, by producing a fiber sensor based on a tapered fiber with a two-layered system formed by of Bismuth film and an Aluminum Oxide, Al_sO_3 (dielectric). The Bismuth layer is a novelty for this kind of devices and provides us with the possibility of studying the performance of a different material, in this case a semimetal . The coatings have been prepared by pulsed laser deposition (PLD), a technique that, given its properties, and specifically the fact that it produces a plasma that is able to embed irregular objects is suitable therefore for deposition of layers on tapered optical fibers.

As it will be shown in more detail later, the accurate determination of the thicknesses of the deposited materials is very important, since the spectral region where the plasmon resonances appear is completely dependent on those. For that reason, to check if the theoretical predictions are in accordance with the obtained experimental results, we need to measure the layers with an advanced technique such as ellipsometry. This is especially important in this case, because we are working with very thin layers of Bismuth (that can present discontinuities and non-uniformity). For that reason, we have characterized the glass substrate used as support for the optical fiber during the layer deposition.

In Section II we depict with more detail the two most relevant aspects of the production of the sensor, namely, the fabrication of the tapered fiber and the deposition of the layers by PLD, starting from the nominal values obtained by the design program developed by us, while in Section III we check the properties of the deposited layers by an ellipsometric study. Finally, in Section IV we perform a refractometric characterization of the device, which shows how plasmon resonances have appeared in the region where they were predicted by the simulation when we take into account the results obtained in the ellipsometric characterization.

II. SENSOR FABRICATION

A. Tapered optical fiber

To produce a DLUWT we use the so-called traveling-burner technique[23]. An optical fiber is gently stretched while heated to achieve a narrowing, thus constituting a taper. The typical profile of a tapered optical fiber is shown in Fig. 1. On the narrowest region, called waist, we deposit a double layer (one metallic, one dielectric) in which the surface plasmon resonance is produced. The mode guided by the fiber enters the taper and is transferred to modes in the newly produced waveguide formed by the air and the cladding (the core almost collapsed and not being capable of supporting any mode). The fact that this technique permits to produce uniform-waist tapers with smooth transitions between regions guarantees that the losses are very low (they are usually called adiabatic tapers). In the waist, the evanescent field is accessible, and can interact with the superstructure that we have deposited. If we adequately calculate the thicknesses of the superimposed materials according to their refractive indices we can achieve a phase-matching between the evanescent field and the plasmon modes existing in the interface between the metallic and the dielectric layers.[24]

We have used a singlemode fiber Newport F-SF and the parameters of the tapers were: waist diameter, 40 μm; waist lenght, 6.34 mm; total length, 28.3 mm.

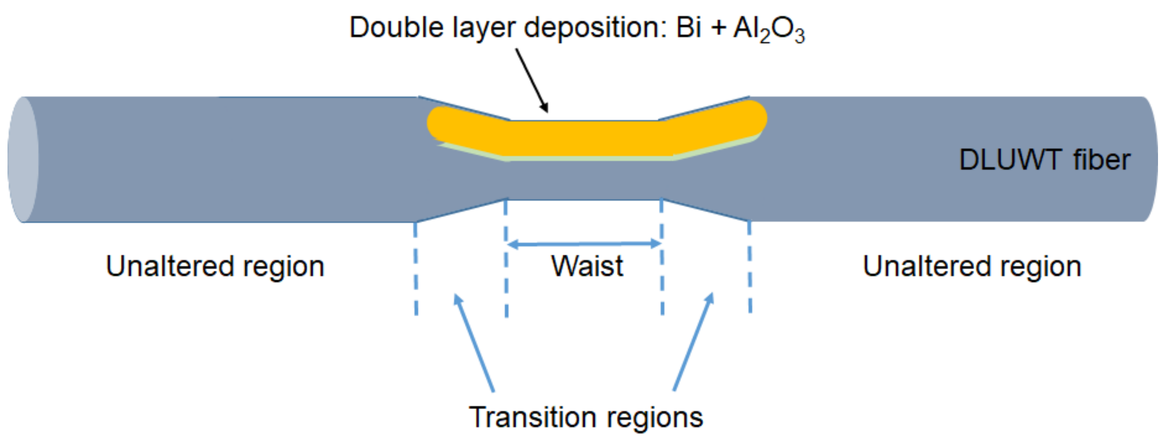

FIG. 1. Schematic representation of the doubly-deposited uniform-waist tapered fiber (DLUWT).

B. Layer deposition

For this study the Bi has been deposited by pulsed laser deposition (PLD) because recent studies have demostrated that this is a suitable technique to obtain Bi films with excellent optical properties[11]. In addition to this, in our PLD system there is an in-situ reflectivity system that allows to follow the evolution of the reflectivity during deposition in order to control the sample thickness[25]. On the other hand, a 360º deposition on a tapered fiber, which is easily obtained with PLD, is very convenient, for it makes plasmon excitation in the sensors independent of polarization.[24] The PLD has been performed using a UV laser ArF excimer (λ = 193 nm, 20 ns pulse duration) and a vacuum chamber equipped with a multi-target system that can accommodate up to four targets. The laser beam is focused at an angle of incidence of approximately 45° onto the targets. BK7 glasses are employed as fiber holders and reference of the deposited films. To fix the fibers to the BK7 glasses, adhesive tape was used. The laser ablation is performed in the on-axis configuration, i.e., the center of the substrate is aligned with the plasma expansion axis. The substrate is rotated during deposition in order to obtain large areas of homogeneous thickness. The films are prepared using an energy density of (1.8 ± 0.2) $J \cdot cm^{-2}$, a pulse repetition of 10 Hz, a target-substrate distance of 45 mm and at room temperature. The experiments were carried out in vacuum at a base pressure of $2 \cdot 10^{-6}$ Torr. A schematic representation of the experiments is shown in Figure 2. To obtain the deposition rates of Bismuth and Al_2O_3, several calibration samples were previously deposited at the same experimental conditions. The rate of deposition depends on the laser energy deposition. For the case of the present article, where the energy density is fixed at (1.8 ± 0.2) $J \cdot cm^{-2}$, the deposition rates are 0.038 nm/s for Al_2O_3 and 0.12 nm/s for Bi. For the fabrication of the films, two commercial Bismuth and Al_2O_3 pure (99.97%) targets were used.

To select the wavelength region where plasmon resonances are going to appear we must determine the adequate thicknesses for the two layers, given that we have adequate knowledge of the refractive indices of the materials. We have been using a quite simple simulation program to design DLUWTs, based on a multilayer matricial calculation, that has proven its effectivity during the years. In this case, as it is discussed in section IV, the challenge was to adapt this scheme to a material that has not been used before for this purpose and that is deposited in a very thin layer. Also the technique of deposition, PLD, is not the usual one for these kind of devices, being PVD and sputtering the most commonly used ones.

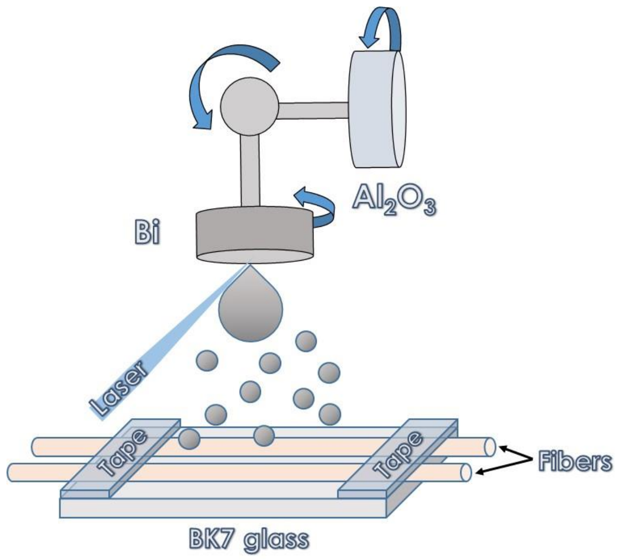

FIG. 2. Schematic representation of the PLD experiments showing the fibers on BK7 glasses.

In this case we selected as nominal thicknesses 9 nm of Bismuth and 90 nm of Al_2O_3 to produce resonances for wavelengths around 850 nm. However, Bismuth, when deposited in thin layers of the order of few nanometers, in the limit of the ultra-thin region, present discontinuities[6,11] and it is more appropriate to speak in terms of effective thickness. It is mainly for this reason that we need the feedback of the ellipsometric characterization. As we will see later, in section IV, when considering the real effective thicknesses deposited, the agreement between the simulation results and the experimentally locations for the resonances is quite good.

III. ELLIPSOMETRIC CHARACTERIZATION

The glass substrate used as support for the optical fibers during the layer deposition, as shown in Figure 2, was characterized using ellipsometry. It can be assumed that the optical properties and thicknesses of the layers on this substrate are similar to the ones over the optical fiber. Nevertheless, it should be noted that we found an appreciable non-uniformity in their thicknesses across the substrate surface.

The ellipsometric measurements were carried out using a Variable Angle Spectroscopic Ellipsometry (VASE) from J.A. Woollam Co. We performed measurements at three incidence angles (65º, 70º and 75º) and a spectral range from 400nm to 1600nm.

Single Bismuth layers deposited by the PLD technique using our setup have been optically characterized in previous works[6] and these values were used for the analysis of the ellipsometric measurements. In this way, we manage the fact that the refractive index and the thickness in the ellipsometric models have a high correlation for thin layers (<100 Å) in the fittings to the experimental data. For Bi the dispersion model is not simple, but can be well described by a generalized oscillator model. The full information can be found in Ref. 11. For the Al_2O_3 we have used a Cauchy dispersion model with $k = 0$ that fits well according to the values of the *Handbook of Optical Constants* by Palik[26].

The model is shown in Figure 3 and it consisted of a glass substrate (previously characterized) with a Bismuth layer and a Bruggeman Effective Medium Approximation layer with Al_2O_3 and voids. Also thickness non-uniformity was included in the model to reproduce the depolarization effect found. This non-uniformity was checked performing additional measurements in different areas of the sample and we found appreciable differences in the ellipsometric parameters and, therefore, in the results from the fittings. This thickness non-uniformity is explained by a bad adherence of the coatings that produced a degradation of the sample. Nevertheless, the results obtained are an enough good estimation to provide the expected spectral location of a plasmon excitation in the SPR fiber sensor as it will be shown in Section IV.

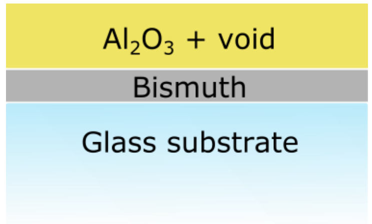

FIG. 3. Scheme of the ellipsometric model used for fitting the experimental measurements.

The results obtained are shown in Table 1 and the fitting plots can be seen in figures 4 and 5.

Mean Squared Error	15.51
Layer 1 thickness: Bismuth	(4.93 ±0.04) nm
Layer 2 thickness: Al_2O_3 + void	(67.8± 0.4) nm
Layer 2 void fraction: Al_2O_3 + void	(23.4 ± 0.7) %
Thickness non-uniformity	(39 ± 1) %

TABLE 1. Fitting results from the ellipsometric measurements

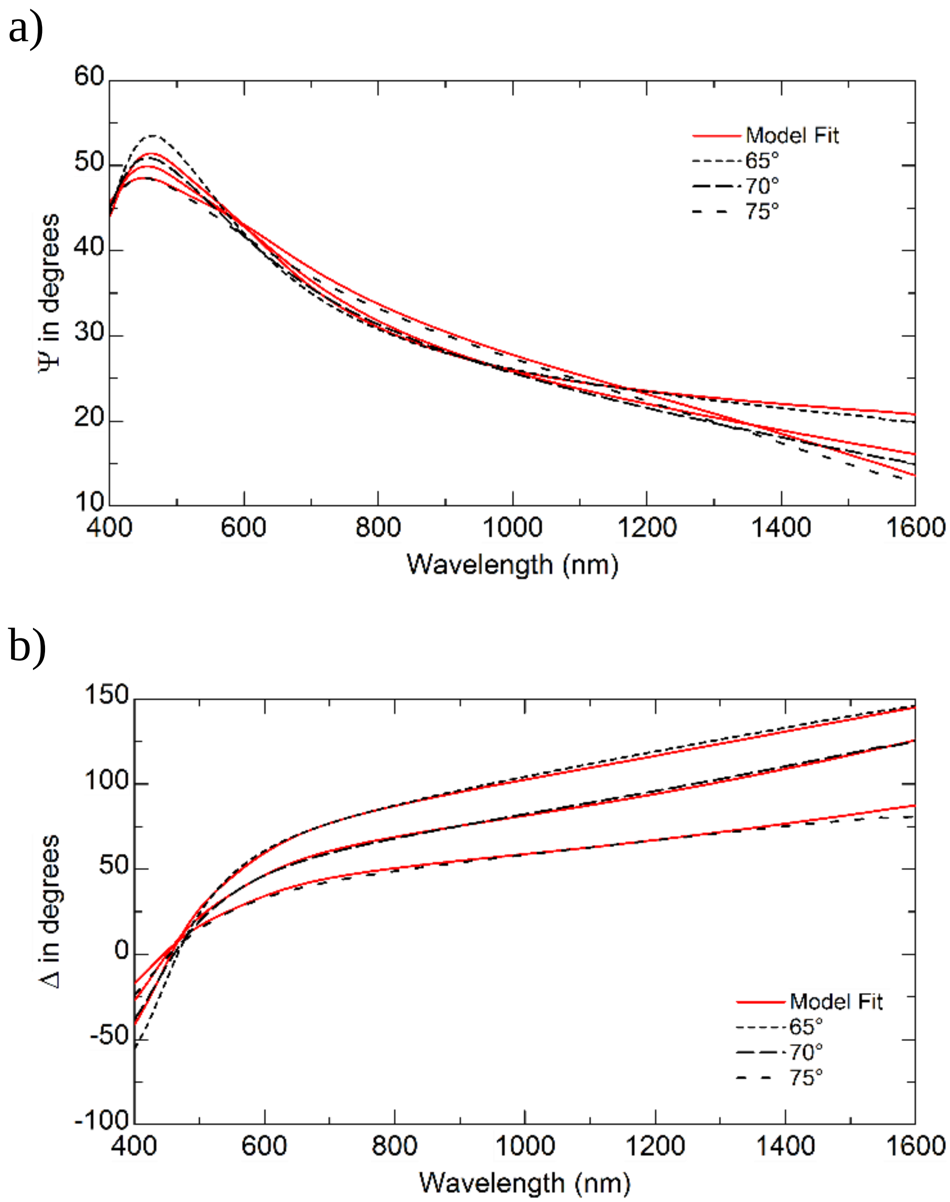

FIG. 4. Fitting plots for the measured Phi (a) and Delta (b) ellipsometric parameters at three angles of incidence (65º, 70º and 75º).

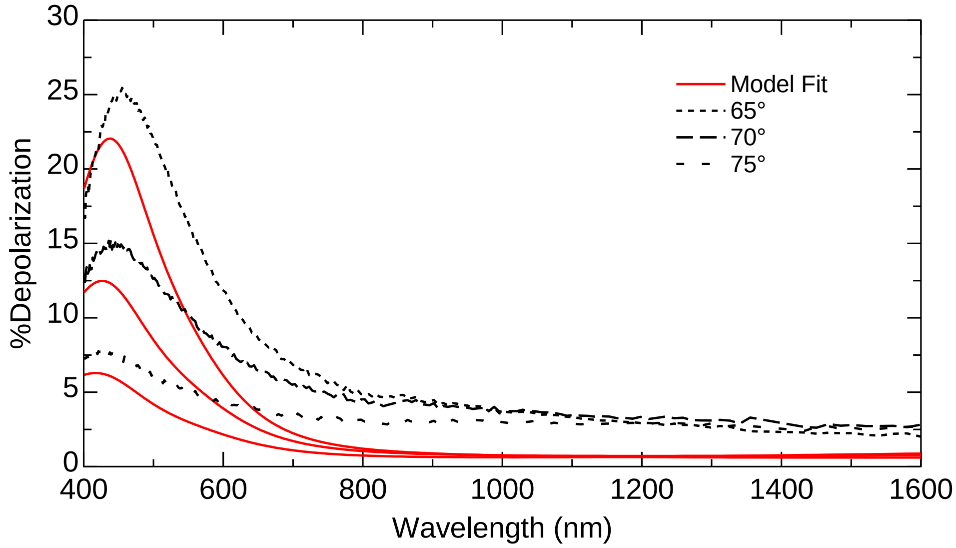

FIG. 5. Fitting plots for the measured depolarization at three angles of incidence (65º, 70º and 75º). This effect is mainly caused by the non-uniformity of the layers.

IV. REFRACTOMETRIC (PLASMONIC) CHARACTERIZATION

A plasmon resonance in this kind of sensors reveals itself as a dip in a transmittance curve, at least in the usual treatment.[25]. This dip is then displaced in a characteristic way when the refractive index of the surrounding medium is changed. That is, SPR sensors are primarily refractometers and we need to perform a refractometric characterization of the system to check if in fact a plasmon excitation has been produced. Since we will be working with spectral interrogation, as it is usual with SPR fiber sensors, there will be a wavelength associated to the plasmon and we are interested in this paper especially in seeing 1) that we have been able to produce SPR in a taper using Bismuth as plasmonic material and 2) that the resonances are in the wavelength region corresponding to the deposited layers and predicted by our model.

To achieve these goals, we have employed our usual characterization procedure[24] (a scheme of the setup is shown in figure 6): the device is submersed in a mixture of water and ethylene glycol, whose index can be changed in a known way by changing the concentration of ethylene glycol. Then, light from a wide-spectrum lamp Avantes Ava-Light-Hal, is launched into the fiber and travels to the sensing region, there interacting with the deposited layers and with the outer medium and eventually exciting plasmons. Finally, light is collected by a spectrometer Avantes AvaSpec-2048-2 and we compute spectral transmittance. As it has been said before, a minimum in transmittance can be associated to a plasmon when the dip is moved if the refractive index of the surrounding medium is changed.

In figure 7 we show a representative result of the ones we obtained with different, similar sensors. We see the whole curve, with different minima that do not displace when the refractive index of the mixture is changed, and one that varies its position: this confirms that we have a plasmon resonance. This is better appreciated in Fig. 8 where we have zoomed the region of the plasmon wavelengths. If we change the index backwards, we observe the similar displacement in the opposite direction, thus making sure that this transmittance minimum effectively corresponds to a plasmon excitation.

We should say that this is not an especially sensitive plasmon as compared with others in the literature. such as the results reported for DLUWTs working with Aluminum as plasmonic material and dielectrics such as TiO_2 and InN. Sensitivity is usually determined as the slope of the curve that corresponds to the variation of the position of the minima when represented against refractive index (that curve is shown in Fig. 9, where a fitting line is drawn for the calculation of sensitivity).

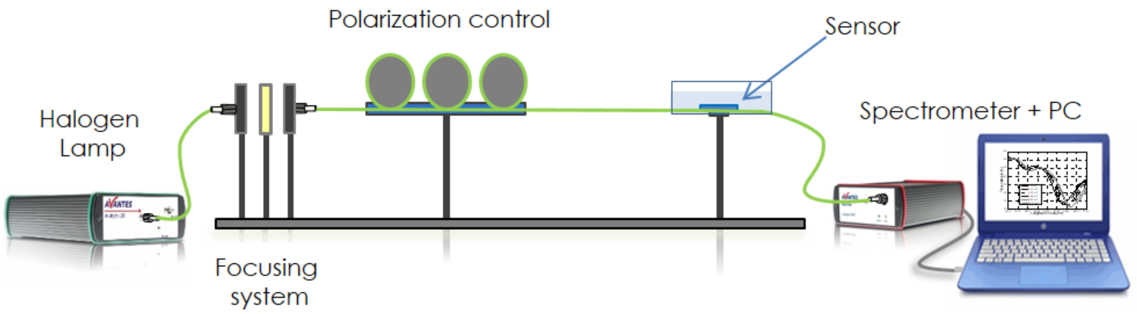

FIG. 6. Setup employed for the refractometric characterization of the sensor.

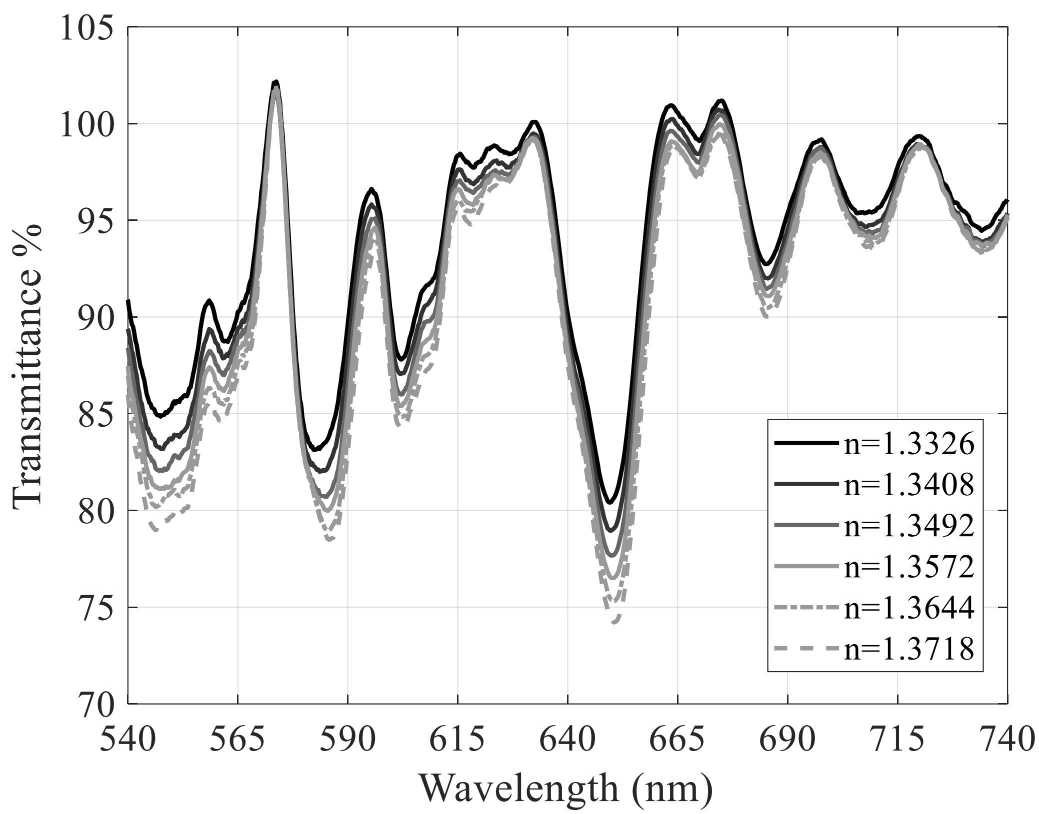

FIG. 7. Spectral transmittance for the sensor when immersed in a medium of variable refractive index. The appearance of values of Transmittance above 100% is a common occurence in this kind of plasmon curves due to the definition of Transmittance, not as a quotient between input and output fluxes, but as the ratio between the signals for the

plasmon excitation and a reference with no plasmon excitation. A thorough discussion of the problem of data processing in SPR sensors can be found in Ref. 27.

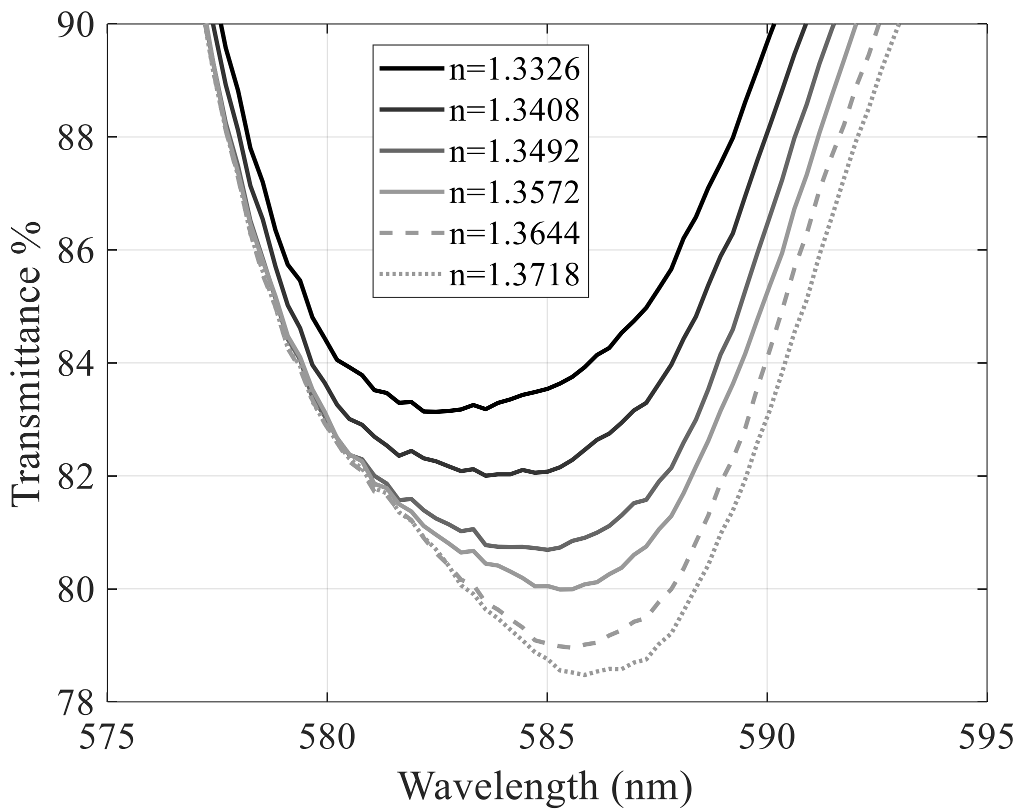

FIG. 8. Zoom of the area of Fig. 7 that corresponds to the plasmonic resonance. The displacement can be appreciated.

In this case we obtain 87 nm/RIU, far from the values of several thousands of nm/RIU that we usually obtain with DLUWTs. However this is an encouraging preliminary result, and further optimization, starting from a better knowledge of the dynamics of deposition of Bi on the fibers, will for sure increase this sensitivity. The differerent capability of Bi as a plasmonic material, in comparison to other usual candidates, as Au or Al, must also be taken into account when comparing sensitivities. In any case, these results prove the feasibility of employing the combination Bi + Al_2O_3 in a DLUWT structure to generate SPR sensors.

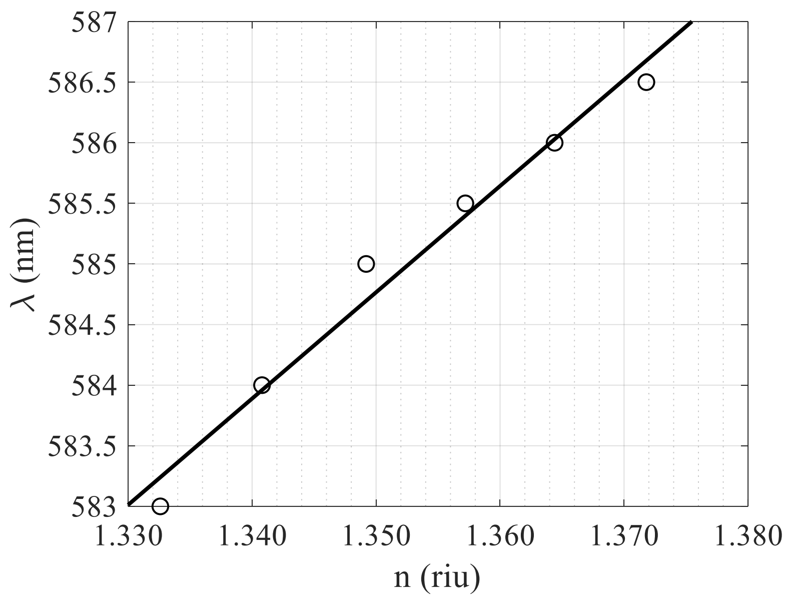

FIG. 9. Position of the minima of Fig. 8 that corresponds to the SPR wavelengths when refractive index varies.

As it has been discussed before, and this is the one of the main subjects of this paper, we needed to check that the obtained experimental results, in terms of plasmon resonances, are in good agreement with the simulated ones. We see that in our spectra the plasmons are shown around 580 - 590 nm, which was not the original region where they were expected. However, if we use the values obtained in the ellipsometric characterization, as depicted in Section III and introduce those thicknesses (around 5 and 68 nm) in the simulation program the prediction of the region of the resonances is greatly improved, as shown in Fig. 10. We see, however, a small deviation, that can obey to the fact that, as it is stated in table 1, the layers thickness is non-uniform. As it has been noted in Section III, there is a significative difference in the values obtained in the different points of the sample, and that sample is not directly the fiber, so one can expect some deviation between the measurements and the real values experienced by the light travelling on the fiber. Taking all this into account, one can say that there is a good agreement between the simulated and the experimental results and that the ellipsometric characterization is of great help for the study of the dynamics of plasmon excitation when using such thin layers of Bismuth.

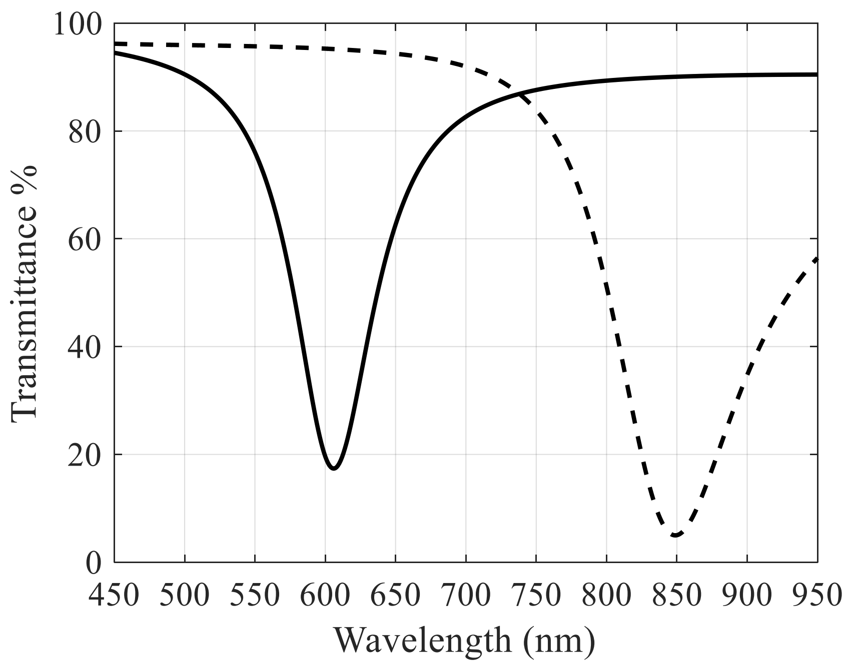

FIG. 10. Comparison between the theoretical predictions for the original intended deposition (dashed line, 9 + 90 nm) and the actual effective thicknesses (continuous line, approximately 5 + 68 nm).

V. SUMMARY AND CONCLUSIONS

In this paper we report the experimental results obtained from a deposition by PLD of a two-layer system formed by a Bismuth thin film and amorphous Aluminum Oxide film over a tapered optical fiber. We show that producing a DLUWT using Bismuth is feasible and that plasmon resonances appear. This is relevant because it opens a new possibility in the design of a novel kind of SPR optical fiber sensors. The use of PLD is suitable for deposition a non-flat surface, such as the curved surface of a fiber, because the laser generated plasma fully embeds the surface. The interesting characteristics of Bismuth and the fact that tor this preliminary study we have only studied a single film thickness suggest that a further study of the dynamics of the deposition and of the response as a function of the film thickness should be performed. The ellipsometric characterization has effectively delivered the necessary information to determine the effective parameters that must be taken into account to evaluate the region of plasmon resonances. As a result a good agreement between simulation and experiment of the fiber sensor response has been achieved.

The incorporation of Bismuth as a plasmonic material to practical devices is a process that it is only in the first stages. Hopefully, this work can contribute to the generation of a new family of SPR fiber sensors based on Bi and with other p-block elements and compound that share common properties.[9-10]

ACKNOWLEDGMENTS

This work has been partially funded by Spanish project RTI2018-096498-B-I00 (MCIU/AEI/FEDER, UE) and by Santander-UCM research project ref. PR75/18-21568. A. Mariscal acknowledges the financial support through BES-2013-062593.

[1]V. I. Petrosyan, V. N. Molin, O. I. Vasin, P. A. Skripkina, S. I. Stenin, and E.G. Batyev, Sov. Phys.-JETP. **39,** 485 (1974).

[2]R. Tediosi, N. P. Armitage, E. Giannini, and D. Van der Marel, Phys. Rev. Lett. **99,** 016406 (2007).

[3]M. Cardona, and D. L. Greenaway, Phys. Rev. **133,** A1685 (1964).

[4]O. Hunderi, J. Phys. F Met Phys. **5,** 2214 (1975).

[5]G. Jezequel, J. Thomas, and I. Pollini, Phys. Rev. B **56,** 6620 (1997).

[6]J. Toudert, R. Serna, and M. Jiménez de Castro, J. Phys. Chem. C **116,** 20530 (2012).

[7]M. Jiménez de Castro, F. Cabello, J. Toudert, R. Serna, and E. Haro-Poniatowski, Appl. Phys. Lett. **105,** 113102 (2014).

[8]A. Cuadrado, J. Toudert, and R. Serna, IEEE Photonics J. **8,** 4801811 (2016).

[9]J. Toudert, and R. Serna, Opt. Mater. Express **6,** 2434 (2016).

[10]J. Toudert, and R. Serna, Opt. Mater. Express **7,** 2299 (2017).

[11]J. Toudert, R. Serna, J. Wojcik, P. Mascher, E. Rebollar, and T. A. Ezquerra, J. Phys. Chem. C **121,** 3511 (2017).

[12]J. Homola, Chem. Rev. **108,** 462 (2008).

[13]P. Singh, Sensor. Actuat. B-Chem. **229**, 110 (2016).

[14]X. Wang, and O. S. Wolfbeis, Anal. Chem. **88**, 203 (2016).

[15]A. K. Sharma, R. Jha, and B. D. Gupta, IEEE Sens. J. **7**, 1118 (2007).

[16]A. González-Cano, M. C. Navarrrete, Ó. Esteban, and N. Díaz-Herrera, Sensors. **14 (3)**, 4791 (2014).

[17]N. Díaz-Herrera, A. González-Cano, D. Viegas, J. L. Santos, and M. C. Navarrete, Sensor. Actuat. B-Chem. **146**, 195 (2010).

[18]M. C. Navarrrete, N. Díaz-Herrera, A. González-Cano, and Ó. Esteban, Sensor. Actuat. B-Chem. **190**, 881 (2014).

[19] Ó. Esteban, F. B. Naranjo, N. Díaz-Herrera, S. Valdueza-Felip, M. C. Navarrrete, and A. González-Cano, Sensor. Actuat. B-Chem., **158**, 372 (2011).

[20]A. González-Cano, F. J. Bueno, Ó. Esteban, N. Díaz-Herrera, and M. C. Navarrete, Appl. Optics **44,** 519 (2005).

[21]E. Rodríguez-Schwendtner, N. Díaz-Herrera, M. C. Navarrete, A. González-Cano, and Ó. Esteban, Sensor. Actuat. A-Phys. **264**, 58 (2017).

[22]E. Rodríguez-Schwendtner, M. C. Navarrete, N. Díaz-Herrera, A. González-Cano, and Ó. Esteban, IEEE Sens. J. **19**, 7355 (2019).

[23]T. A. Birks, and Y. W. Li, J. Lightwave Technol. **10**, 432 (1992).

[24]M. C. Navarrete, N. Díaz-Herrera, A. González-Cano, and Ó. Esteban, Plasmonics. **5**, 7 (2010).

[25]R. Serna, A. Suárez-García, C.N. Afonso and D.Babonneau, Nanotechnology **17** , 4588 (2006).

[26]E.D. Palik (ed.), *Handbook of Optical Constants of Solids*, Academic Press, 1997.

[27]E. Rodríguez-Schwendtner, A. González-Cano, N. Díaz-Herrera, M. C. Navarrete, and Ó. Esteban, Sensor. Actuat. B-Chem. **268**, 150 (2018).

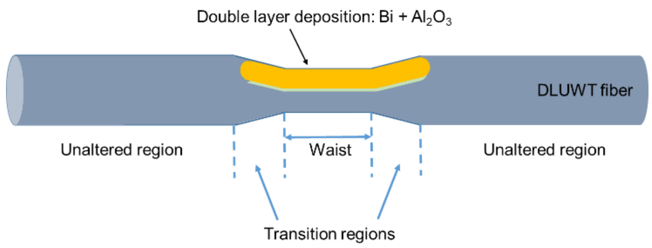
Double layer deposition: Bi + Al_2O_3
DLUWT fiber
Unaltered region
Waist
Unaltered region
Transition regions

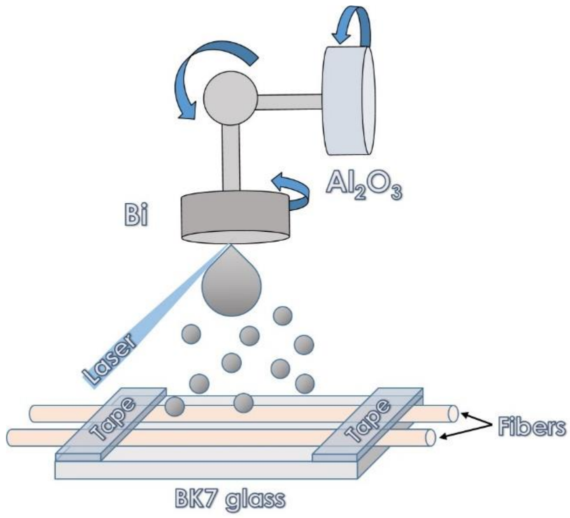
Al2O3
Bi
Laser
Tape
Tape
Fibers
BK7 glass

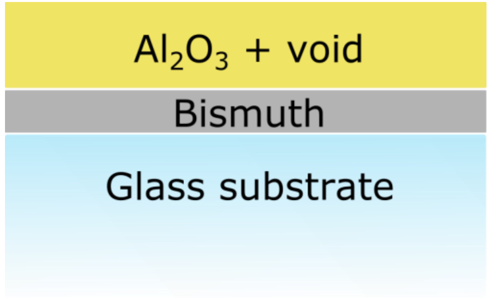
Al_2O_3 + void
Bismuth
Glass substrate

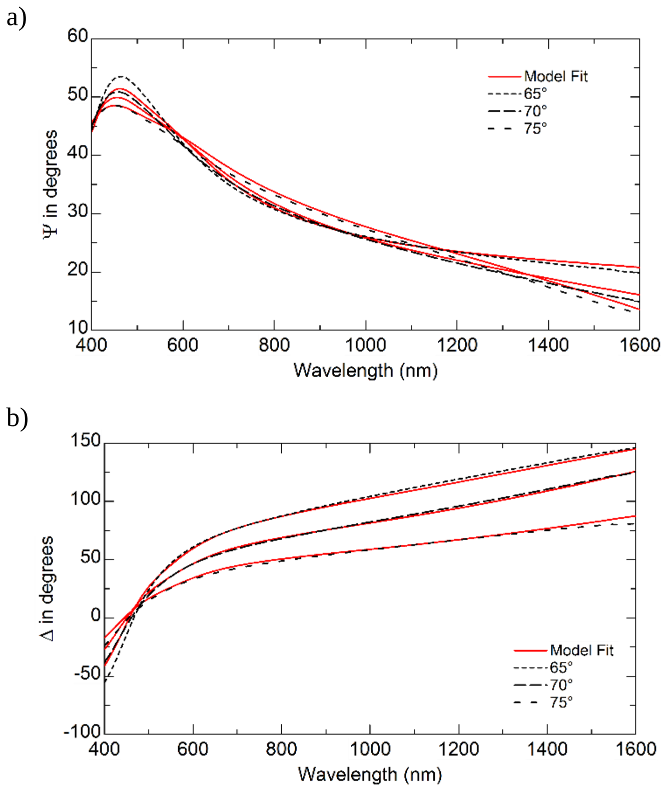
a)
Ψ in degrees
Wavelength (nm)
Model Fit
65°
70°
75°
b)
Δ in degrees
Wavelength (nm)
Model Fit
65°
70°
75°

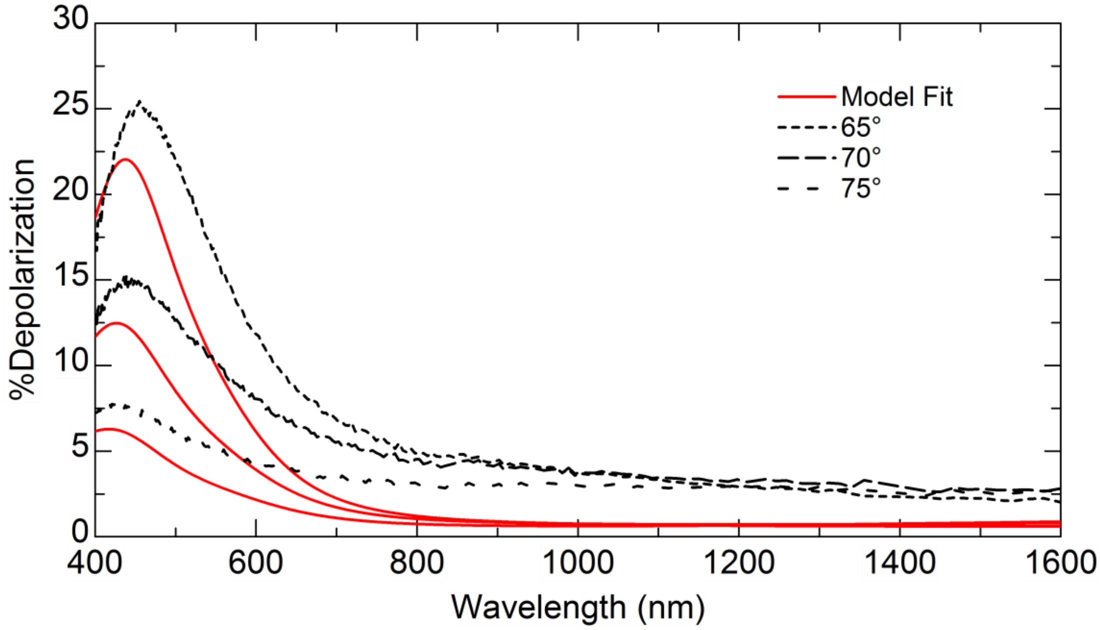
%Depolarization
Wavelength (nm)
Model Fit
65°
70°
75°
0
5
10
15
20
25
30
400
600
800
1000
1200
1400
1600

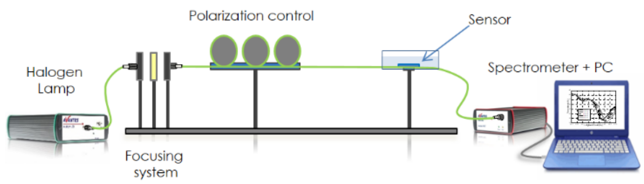
Polarization control
Sensor
Halogen
Lamp
Spectrometer + PC
Focusing
system

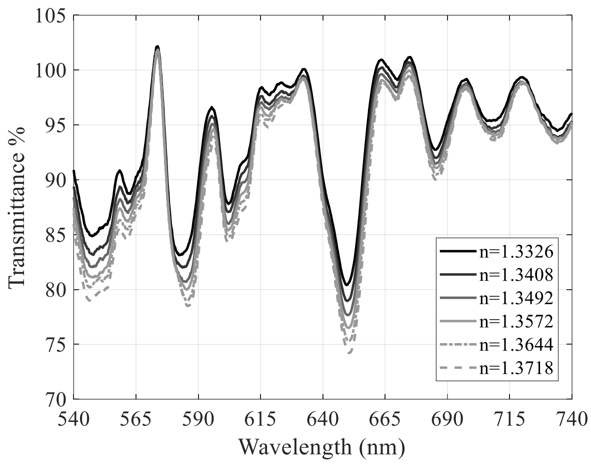
Transmittance %
Wavelength (nm)
105
100
95
90
85
80
75
70
540
565
590
615
640
665
690
715
740
n=1.3326
n=1.3408
n=1.3492
n=1.3572
n=1.3644
n=1.3718

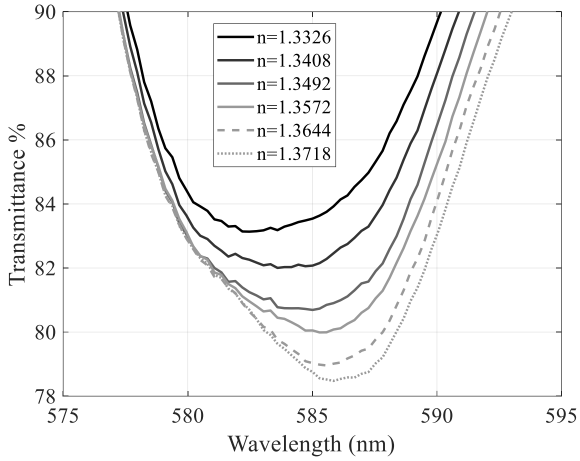
n=1.3326
n=1.3408
n=1.3492
n=1.3572
n=1.3644
n=1.3718
Transmittance %
Wavelength (nm)
90
88
86
84
82
80
78
575
580
585
590
595

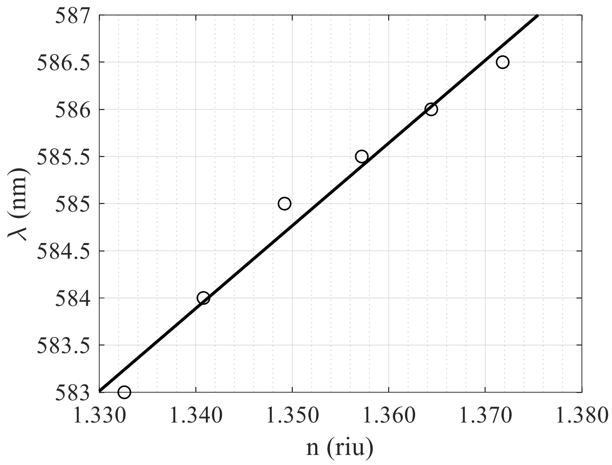
λ (nm)
587
586.5
586
585.5
585
584.5
584
583.5
583
1.330
1.340
1.350
1.360
1.370
1.380
n (riu)

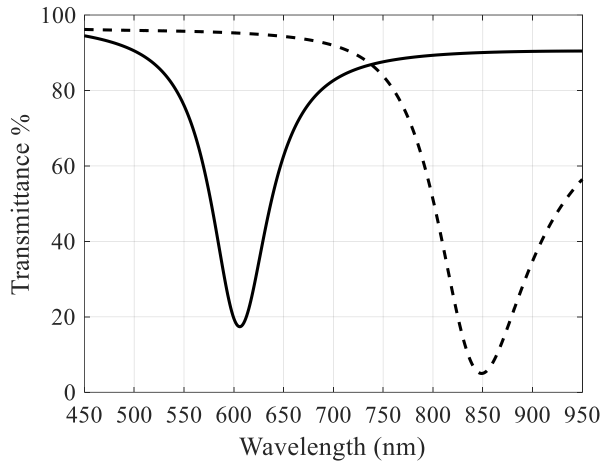
Transmittance %
100
80
60
40
20
0
450 500 550 600 650 700 750 800 850 900 950
Wavelength (nm)